1	Discovery of unusual dimeric piperazyl cyclopeptides encoded by a <i>Lentzea flaviverrucosa</i> DSM				
2					
	44664 biosynthetic supercluster				
3					
4	Chunshun Li, a,b,e,#, Yifei Hu ^{c,f,#} , Xiaohua Wu ^a , Spencer D Stumpf ^{c,g} , Yunci Qi ^c , John M				
5	D'Alessandro ^{c,h} , Keshav K Nepal ^c , Ariel M. Sarotti ^d , Shugeng Cao ^{a,b,*} , Joshua AV Blodgett ^{c,*}				
6					
7 8 9 10 11 12 13 14 15 16 17 18 19	^a Department of Pharmaceutical Sciences, Daniel K. Inouye College of Pharmacy, University of Hawaii at Hilo, 200 West Kawili Street, Hilo, HI 96720.				
	^b Cancer Biology Program, University of Hawaii Cancer Center, 701 Ilalo Street, Honolulu, HI 96813.				
	^c Department of Biology, Washington University in St Louis. 1 Brookings Drive, St Louis MO 63122.				
	^d Instituto de Química Rosario (CONICET), Facultad de Ciencias Bioquímicas y Farmacéuticas, Universidad Nacional de Rosario, Suipacha 531, Rosario 2000, Argentina.				
	*Denotes equal contribution to this work.				
20	*Corresponding Authors:				
21	Shugeng Cao, scao@hawaii.edu orcid.org/00000-0001-6684-8221				
22	Joshua Blodgett, jblodgett@wustl.edu orcid.org/0000-0002-7080-5870				
23 24 25 26 27 28 29	Present addresses:				
	^e Antheia, Inc., 1430 Obrien Dr, Menlo Park, CA 94025				
	^f Pritzker School of Medicine, The University of Chicago, Chicago, IL 60637				
	^g Pfizer Inc, 875 Chesterfield Pkwy W, Chesterfield, Missouri 63017				
30	^h Animal Sciences Research Center, University of Missouri, Columbia, MO 65211				
31					
32	Classification: Microbiology & Chemistry				
33					
34 35	Keywords: rare actinomycete, <i>Lentzea</i> , piperazate, biosynthesis, cyclopeptide, cytochrome P450				
36					

Abstract:

37

38

39

40

41

42

43

44

45

46

47

48

49

50

51

52

53

54

55

56

57

58

59

60

61

Rare actinomycetes represent an underexploited source of new bioactive compounds. Here, we report the use of a targeted metabologenomic approach to identify new piperazyl compounds in the rare actinomycete Lentzea flaviverrucosa DSM 44664. These efforts to identify molecules that incorporate piperazate building blocks resulted in the discovery and structural elucidation of two dimeric biaryl-cyclohexapeptides, petrichorins A and B. Petrichorin B is a symmetric homodimer similar to the known compound chloptosin, but petrichorin A is unique among known piperazyl cyclopeptides because it is an asymmetric heterodimer. Due to the structural complexity of petrichorin A, solving its structure required a combination of several standard chemical methods plus in silico modeling, strain mutagenesis, and solving the structure of its biosynthetic intermediate petrichorin C for confident assignment. Furthermore, we found that the piperazyl cyclopeptides comprising each half of the petrichorin A heterodimer are made via two distinct non-ribosomal peptide synthetase (NRPS) assembly-lines, and the responsible NRPS enzymes are encoded within a contiguous biosynthetic supercluster on the L. flaviverrucosa chromosome. Requiring promiscuous cytochrome p450 crosslinking events for asymmetric and symmetric biaryl production, petrichorins A and B exhibited potent in vitro activity against A2780 human ovarian cancer, HT1080 fibrosarcoma, PC3 human prostate cancer, and Jurkat human T lymphocyte cell lines with IC50 values at low nM levels. Cyclic piperazyl peptides and their crosslinked derivatives are interesting drug leads, and our findings highlight the potential for heterodimeric bicyclic peptides such as petrichorin A for inclusion in future pharmaceutical design and discovery programs.

Significance:

Actinomycetes produce many clinically-useful drugs, especially antibiotics and anticancer agents. Rare actinomycetes are known to produce bioactive molecules, but they remain

underexplored compared to more-common *Streptomyces spp*. Natural molecules having piperazate building-blocks are often bioactive, and genome analyses previously indicated the rare actinomycete *Lentzea flaviverrucosa* DSM 44664 may encode for the production of such molecules. To discover these from complex fermentation mixtures, we devised and employed a targeted metabolomic approach that revealed petrichorin A, an unusual heterodimeric biaryl-cyclohexapeptide. Its structure was determined by using multi-dimensional NMR, theoretical calculations, and strain mutagenesis, and its biosynthesis implicated an atypical cytochrome p450 heterodimerization event. Petrichorin A demonstrated potent cytotoxicity, highlighting heterodimeric-biaryls as interesting features for future drug design.

Introduction:

Nature represents one of humankind's most important and enduring sources of therapeutics. The ability of living things to produce drug-like compounds is unevenly distributed in biology, where certain types of organisms are particularly enriched (1). Filamentous actinomycete bacteria are particularly noteworthy for this trait, producing >50% of molecular scaffolds found in clinically-utilized antibiotics plus many other needed medicines (2). Drug discovery from actinomycetes and other microbes has seen a great revitalization in recent years (3). While the roots of this revitalization are complex, a combination of emerging drug scarcity, changing attitudes towards microbial bioproduction, and renewed enthusiasm for evolved molecules as drug leads were significant drivers (4).

Demands for new antibiotics are critical, with resistant and emerging infections posing a serious but largely unchallenged global health threat (5). The idea that actinobacterial products might have future roles in mitigating that threat owes primarily to the advent of increasingly affordable DNA sequencing and the development of advanced genomics toolsets (6, 7). Once thought to be largely devoid of new drugs, these technologies revealed a deep trove of yet-undiscovered drug-like molecules hidden in actinobacterial genomes (8).

However, translating genomic knowledge into molecules for clinical development has proved to be challenging (9). Many biosynthetic gene clusters (BGCs) that encode desirable molecules are thought to be "silent" (10). Silent clusters are characterized by the lack of expected chemical products, which frustrates drug development efforts. Furthermore, the computational side of drug discovery [i.e., genome sequencing, annotation, and biosynthetic prediction] now vastly outpaces the experimental capacity to prosecute all newly discovered BGCs for molecule discovery. Because of this, discovery requires the use of increasingly complex schemes to identify which bacterial strains and biosynthetic loci will most likely produce desirable molecules once pursued (7, 11). Bioinformatic efforts typically scan microbial genomes for BGCs encoding molecules having known pharmacophores, privileged scaffolds, or other desirable chemical motifs. Microbial producers are selected for genome-sequencing based on equally complex criteria, including their relatedness to traditional producers of approved drugs, isolation from unique environmental niches, their relative rarity in culture collections, and other factors (12).

Piperazate (piz) is a non-proteinogenic amino acid and proline mimic that imparts conformational constraint and other desirable properties to natural and synthetic molecules that incorporate it (13). Piz fits the classical definition of a privileged scaffold, a molecular substructure associated with compounds that can target diverse biology (14). Thus, piperazyl compounds are desirable for therapeutic discovery. In addition to being counted among several known drugs and important structural leads [e.g., cilazapril, the matlystatins, and sanglifehrins (15)], piperazyl molecules have additional research interest owing to their atypical associated enzymology (16-18) and proposed roles in microbial symbiosis and chemical ecology (19-21).

There are over 100 documented natural products with integral piz moieties, most of which are produced by actinobacterial members of the *Streptomyces* genus (22). The recent elucidation of piz biosynthesis via the unusual hemoprotein KtzT and related members of the PzbB-protein family has enabled straightforward recognition of piperazyl-molecule BGCs in

microbial genomes (17, 18). Our prior work on actinobacterial piperazate metabolism revealed a pzbB-linked BGC in Lentzea flaviverrucosa DSM 44664, and the enzyme it encodes was competent for piperazate production in heterologous Streptomyces hosts (18). L. flaviverrucosa is a member of the Pseudonocardia family, and is a member of the so-called "rare actinomycetes" (23). Rare actinomycetes, including Lentzea, Actinoplanes, Nonomurea, Salinispora plus several other genera, are phylogenetically-diverse and biotechnologicallyinteresting filamentous actinobacteria (23). These organisms are recognized for their potential to produce biotechnologically important molecules, but remain significantly underexplored compared to their more commonly encountered Streptomyces relatives (24). Understanding and accessing the biosynthetic potential of rare actinomycetes is a priority for continued natural drug discovery, but work exploring Lentzea for biotechnology remains relatively sparse. Known Lentzea products include rebeccamycin (25), lassomycin (26) and the lentzeosides (27), and members of the genus have been used for the bioconversion of the cyclosporin A-derivative FR901459 into several new congeners (28). Published examples of Lentzea genetic systems to support biotechnological development are also limited, with Lentzea. sp. strain ATCC 31319 mutations for the study of thiolactomycin production being the lone example (29).

Motivated by our earlier findings indicating *L. flaviverrucosa* should produce a yet-undiscovered piperazyl compound (18), here we report the targeted discovery of the biosynthetically atypical piperazyl compounds petrichorins A and B (Fig. 1) from this strain. Identifying these molecules in growth extracts was enabled by a combination *pzbB* gene disruptions, *L*-orn isotopic-labelling, and piperazyl-targeting MS/MS fragmentation analysis. After fully resolving their structures, both petrichorins were found to share several structural features with a growing family of cyclic peptides and depsipeptides [including chloptosin (30), himastatin (31), and members of the alboflavusin (32, 33) and kutzneride (34) complexes, (Fig. 1, top)] that incorporate both piperazyl and hydroxyhexahydropyrrolo[2,3-*b*]indole-2-carboxamide (HPIC) substructural elements. Of the two petrichorins, the minor product

petrichorin B was more structurally simplistic, consisting of a bicyclic-cyclopeptide homodimer whose structure is highly similar to chloptosin. By comparison, the major product petrichorin A significantly differed from all previously known dimeric cyclohexapeptides in that it is a heterodimer comprised of one half of petrichorin B crosslinked to a different cyclohexapeptide, named petrichorin C (Fig. 1, bottom). The biosynthesis of the petrichorins was pursued via additional genetic experiments in the native host, revealing that the production of the highly-atypical asymmetric dimer petrichorin A requires an unusual cytochrome p450 crosslinking of two different cyclopeptides generated by distinct NRPS assembly lines. Finally, the bioactivites of petrichorins A, B, and C were tested against human HT1080 fibrosarcoma, PC3 prostate cancer, and Jurkat T lymphocyte cell lines. The petrichorin A heterodimer showed significant inhibition along with the B homodimer, and both of these were superior to the C monomer. Accordingly, we posit that heterodimeric biaryl-cyclohexapeptides and their depsipeptide analogs should be specifically considered for future therapeutic-lead synthesis.

Results and Discussion:

Piperazate-targeted Metabologenomics for Petrichorin Discovery. Piperazate biosynthesis requires the formation of an unusual N-N bond, which is formed by heme b-dependent enzymes related to KtzT. We previously identified and heterologously expressed a *ktzT* ortholog from *L. flaviverrucosa* (*ltzT*) that produces piperazate in recombinant *Streptomyces lividans* and *Streptomyces flaveolus* (18). This suggested that *L. flaviverrucosa* likely has the native capacity to produce piperazyl compounds, but none had been discovered in this strain or in any other *Lentzea spp.* Examining the *ltzT* gene neighborhood revealed a potential biosynthetic gene cluster (BGC, ~67 kb, *ltzA-ltzV*) encoding multiple predicted tryptophan halogenases, five NRPS enzymes having 11 total adenylation domains, a single transcriptional regulator, transporters, and several oxidative tailoring genes (Fig. 2A, Table S1).

To discover piperazyl molecules in L. flaviverrucosa, we used a multipronged approach based on the genetics of piz monomer production and piperazate-targeted metabolomics (Fig 2B-D). Piz biosynthesis from L-ornithine (L-orn) requires an N-hydroxylase and an N-hydroxy-L-orn cyclase, and homologs of both were found in the Itz locus (Fig 2A, ItzF and ItzT, respectively). Thus, we tested L. flaviverrucosa for a metabolic response to exogenous L-piz and d^T -L-orn to identify potential piperazyl compounds. After feeding the strain with these amino acids, organic extracts of spent growth media were analyzed via LC/MS, revealing a single strong peak that responded positively to both compounds (Fig. 2B-C). Specifically, exogenous L-Piz approximately doubled the peak area of one L. flaviverrucosa metabolite (0.5- 1 mM supplementation) and the same piz-responsive signal also incorporated deuterated-L-orn, consistent with a piperazyl metabolite.

We then utilized an MS/MS fragmentation scheme for more sensitive detection of piperazyl compound signals within complex microbial extracts. This method was established using matlystatin production in *Amycolatopsis atramentaria* (35, 36), where MS/MS was used to identify daughter ions containing the piperazyl-feature of matlystatin B via d^7 -L-Orn incorporation (Fig S1). By comparing labelled vs unlabeled extracts, we identified a piperazate-derived m/z 85.1 fragment, which we surmised could be used for the sensitive detection of other piperazyl compounds. After applying this method to *L. flaviverrucosa*, we re-discovered the piz-responsive signal from Fig. 2B, plus an additional minor product missed by our initial efforts (Fig. 2D).

To confirm these molecules are indeed piz-dependent and encoded by the *Itz* locus, we established a genetic system in *L. flaviverrucosa* to create unmarked gene deletions. This was achieved using a standard *rpsL*-counterselection approach (see Methods), and all mutants described herein were created in the same *rpsL* background (S12 K88M, JV691). After deleting piz-essential *ItzT*, the resulting mutant was deficient for both peaks identified in Fig. 2D. Both signals were rescued by ectopically-expressing *ItzT* under the control of the strong constitutive promoter PermE*. Other *ItzT* orthologs cloned from piperazyl BGCs in *Kutzneria* sp strain 744

(ktzT, kutznerides) and Streptomyces himastatinicus (hmtC, himastatin) similarly restored function (Fig. 2D). These data clearly linked the production of the Fig. 2 piperazyl signals to the Itz locus.

191

192

193

194

195

196

197

198

199

200

201

202

203

204

205

206

207

208

209

210

211

212

213

214

215

216

Structure of the Petrichorins. Both molecules detected in Fig. 2D were purified to homogeneity for structural elucidation (see Methods and SI Appendix). Both were isolated as white powders, and HR-ESI-MS revealed each had distinct masses and mass formulae [the major product, petrichorin A, $C_{67}H_{92}CI_2N_{18}O_{18}$ m/z 1507.6288, calcd for [M + H]⁺ 1507.6287; the minor product petrichorin B, $C_{70}H_{98}CI_2N_{18}O_{20}$ quasi-molecular ion peak at m/z 1603.6484 [M + Na]⁺, calcd 1603.6474].

NMR characterization of petrichorin A was challenging due to extensive signal overlap. Pursuing the final structure of this molecule thus required a combination of standard 1D and 2D NMR and other chemical methods (Supplementary Data and Table S2), plus in silico modeling and strain mutagenesis for confident structural assignment (latter discussed below). In brief, comprehensive 2D-NMR analysis (COSY, TOCSY, HSQC, and HMBC, Figs S2-S8) suggested the presence of one alanine (ala), one N-methyl-alanine (NMe-ala), one isoleucine (ile), one Omethyl-serine (OMe-ser), two threonines (thr-1 and thr-2), four piperazic acids [one being hydroxylated at γ -position], plus two chlorinated tryptophan (trp) derivatives [later identified as HPIC]. Amino acid hydrolysis followed by Marfey's analysis (37) indicated the absolute configuration of the component amino acids (Figs S9-S16), and HMBC and NOESY were used to determine amino acid sequences for both the asymmetric left and right rings of petrichorin A (Fig S28). Additionally, Mosher reactions coupled with 2D NMR (38) were used to determine the absolute configuration of secondary alcohols (Figs S17-27). Finally, the absolute configurations of the asymmetrically chlorinated and cross-linked HPIC residues of heterodimeric petrichorin A required quantum calculations of NMR shifts, an established strategy to resolve difficult natural product structures (39). To do this with minimized computational cost, we theoretically modeled four simplified bicyclic HPIC derivatives (Fig S29 1a-d, and Fig S30) and correlated calculated

shifts with collected experimental values for the analogous region of petrichorin A. Following systematic conformational sampling at the MMFF level, followed by fast NMR calculations at B3LYP/6-31G** the *J*-DP4 calculations suggested Fig. S29- **1a** as the most likely substructure (99.97% confidence) (40). This result further verified by DP4+ (>99.99% confidence) after refining the NMR calculations at the PCM/mPW1PW91/6-31+G**//B3LYP/6-31G* level of theory (see Tables S5-6 and accompanying diagrams) (41). From these summed experiments, petrichorin A was revealed to be a unique asymmetric dicyclohexapeptide, comprised of two distinct piperazyl cyclopeptides tethered by a biaryl linkage as shown in Fig. 1 (see *SI Appendix* for further data and detail).

Solving the molecular structure of petrichorin B was relatively straightforward compared to petrichorin A, owing to its symmetric, homodimeric structure. Following a similar battery of 1D and 2D NMR, hydrolytic component analysis, derivatization and theoretical NMR calculations used for petrichorin A (Supplementary Data, Tables S3, S7-8, Figs S28, S33-S46) petrichorin B was found to consist of a symmetric homodimer of the same cyclopeptide that constitutes the left ring of petrichorin A (Fig. 1). While heterodimeric petrichorin A was unique in the chemical literature, petrichorin B was found to be highly similar to chloptosin (30). The only significant differences between them were that petrichorin B substitutes *allo*-isoleucine for chloptosin's valine, and petrichorin B has two γ -hydroxyl-piz moieties while all chloptosin piz residues are non-hydroxylated.

NRPS assembly of the Petrichorins. The clear structural parallels that exist between petrichorin B and chloptosin suggested they likely arise from highly similar pathways, but the chloptosin BGC remains unreported in the literature, making it unavailable for comparison. While the *Itz* locus remains architecturally-distinct in online sequence databases, published BGCs for the biosyntheses of the piperazyl cyclodepsipeptides himastatin and kutzneride from *Streptomyces himastatinicus* ATCC 53653 and *Kutzneria* sp. strain 744 respectively (Fig. S47)

share partial parallels with the *ltz* locus with regards to gene content and organization. However, the *ltz* locus critically lacks genes for the polyketide enzymology needed for depsipeptide linkages and their associated biosynthetic intermediates, which are integral to the kutznerides and himastatins.

243

244

245

246

247

248

249

250

251

252

253

254

255

256

257

258

259

260

261

262

263

264

265

266

267

268

The different peptide sequences making up each ring of the petrichorin A heterodimer [left ring: D-allo-ile, L-Piz, D-(4S-OH)-piz, L-O-methyl-ser, D-thr, L-6-Cl-HPIC; right ring: D-ala, L-piz, D-thr, L-N-methyl-ala, D-piz, L-7-Cl-HPIC] indicated each half of the molecule must be synthesized via distinct NRPS enzymology. Assigning which Itz-associated NRPS genes are responsible for petrichorin A and B biosyntheses initially involved bioinformatic analysis of the Itz cluster's NRPS enzymes to predict the order and chirality of possible peptide products (Table S9). These data led us to posit that an NRPS assembly line consisting of LtzDE most likely directs the precursor of the left ring of petrichorin A (Fig 1 and Fig 3). Due to obvious structural parallels, this also implicates LtzDE in the production of homodimeric petrichorin B (Fig 1). Concordantly, the assembly line comprised of LtzUV showed substantial collinearity with the expected peptide precursor of the right ring of petrichorin A. O-methyltransferase and Nmethyltransferase domains found within NRPS proteins are readily discernable from each other by sequence (42), and single-instances of these domains were respectively found within LtzE and LtzV. Their placement within each NRPS assembly-line dovetailed seamlessly with the rest of our molecular co-linearity analyses. Finally, the presence of several epimerization domains within both NRPS assembly lines agreed with the actual structures of the petrichorins wherever D-configured amino acids were encountered (Fig. 3).

However, we noted both of the LtzDE and LtzUV assembly lines deviate from standard NRPS domain orders because each is missing a contextually-expected adenylation domain (Fig 3; LtzE module 3 and LtzV module 1). After comparing the domain orders of these assembly lines against the amino acids that comprise both petrichorins, the most parsimonious explanation is that LtzA [predicted to activate *L*-thr] must functionally replace both of these

missing adenylation domains. Thus, LtzA likely acts as a trans-modular NRPS enzyme, partnering with both LtzDE and LtzUV. While *trans*-acting NRPS adenylation modules remain fairly scarce in the literature, several examples are now documented (46). Furthermore, the kutzneride pathway requires one (47), and homology suggests one is likely to function in himastatin (31) production as well [HmtL module 6 is missing a necessary adenylation domain, and HmtF shares the same X-A-T domain order as LtzA].

To determine which NRPS assembly line(s) function in petrichorin A and B production, $\Delta ItzU$ and $\Delta ItzD$ mutations were created and the accumulation of piperazyl peptides were monitored by LC/MS/MS (Fig. 4). Deleting ItzU abrogated heterodimeric petrichorin A production, but not the homodimer petrichorin B, which agrees with precursor production model in Fig 3. In contrast, deleting ItzD lost all dimeric cyclohexapeptide production. Instead, the strain accumulated a molecule with a mass consistent with a monomeric cyclopeptide. Once purified to homogeneity and structurally characterized [essentially as done for petrichorins A and B; Table S4, Figs S28, S48-S55], this biosynthetic intermediate (petrichorin C) was confirmed as being equivalent to one-half of the petrichorin A heterodimer [Fig 1 legend]. In addition, the simplified NMR spectra obtained for petrichorin C were used to further strengthen the initial NMR interpretations of the corresponding subregion of petrichorin A. We found it curious that we were unable to detect the theoretically-possible dimer of petrichorin C in the ItzD mutant, while the homodimer petrichorin B was readily produced in the ItzU strain. The reason why the latter homodimer is readily produced while the other one apparently isn't remains unknown.

Finally, the above analyses suggested that most of the biosynthetic building blocks required for NRPS-elaborated precursor peptide formation are either supplied via central metabolism through standard proteinogenic amino acid pools, or are produced by enzymes encoded within the cluster itself (ie, piperazate, *ltzF* and *ltzT*). The single exception to this was *L-allo-*ile, likely activated by LtzD module 1. *L-allo-*ile is known to be produced from *L-*ile in a pyridoxal phosphate-dependent, two-enzyme pathway that requires enzymes homologous to

MfnO/DsdD and MfnH/DsaE (48). Missing from the *Itz* locus, searching the *L. flaviverrucosa* genome with MfnO and MfnH from the marformycin (49) cluster identified homologs (WP_090070987.1 and WP_090064152.1, respectively) encoded outside of the petrichorin supercluster that could potentially be involved in *allo*-ile production.

Cytochrome P450 involvement in petrichorin (hetero)dimer formation and tailoring. Multiple cytochrome P450 enzymes encoded within the chloptosin, himastatin, kutzneride, and alboflavusin biosynthetic loci are known to be involved in the maturation of tryptophan into HPIC [KtzM, HmtT, AfnD], piperazyl peptide oxidation [HmtN and AfnA], and the formation of homodimeric (chloro)biaryl crosslinkages between HPIC residues [HmtS and ClpS] (30-32, 47, 50). While these transformations have been investigated elsewhere, we probed the functions of their homologs encoded within the *ltz*-locus [LtzR, LtzS and LtzH, respectively; Fig 5.] for multiple reasons. These include a general difficulty in predicting biosynthetic P450 functions from sequence similarity alone (51), and LtzR, LtzS and LtzH are all members of the same P450 family [CYP113, using CYPED (52)]. Furthermore, *Lentzea* affords an interesting opportunity to study these P450s within the context of a seldom-studied rare actinomycete host. Finally, none of the other pathways yield heterodimeric products, necessitating further investigation.

While limited numbers of P450s sourced from characterized piperazyl-HPIC cyclopeptide BGCs are available for comparison, we employed a Maximum-Likelihood inferred phylogeny (Fig. 5A) of the proteins above and their *Itz*-locus encoded homologs to assess if an evolutionary approach might better guide functional prediction. We found P450s involved in HPIC formation (blue highlights) and HPIC-biaryl crosslinking (red highlights) formed monophyletic groups, and LtzR and LtzS respectively claded within those groups. However, LtzH formed a separate group with HmtN, a piperazyl-peptide hydroxyating P450 from the himastatin (31) pathway, and these were polyphyletic with AfnA [a P450 thought to have a similar function as HmtN(32)]. Together, this suggested that biaryl linking and HPIC forming

P450s might be discernable using molecular phylogeny, but that piz-cyclopeptide hydroxylating P450s may have complex ancestry that complicates *in silico* identification.

From this, we inferred that LtzR is likely involved in petrichorin HPIC formation, LtzS is required for cyclopeptide crosslinking, and that LtzH is involved in piperazyl hydroxylation [by virtue of its similarity to HmtN and the presence of *D*-(4-OH)-Piz subunits in both petrichorins]. After constructing unmarked deletion mutants in *ltzR*, *ltzS* and *ltzH*, we found that each strain accumulated several biosynthetic intermediates having retention times and masses distinct from petrichorin A and B. In concert with the phylogenetic predictions and previous himastatin biosynthesis and engineered alboflavusin dimerization analyses, we predicted that a Δ*ltzR* strain should be unable to produce crosslinked intermediates based on the inability of the strain to produce HPIC (where intact HPIC is apparently necessary for downstream P450 crosslinking) (32). Our high-resolution MS and LC/MS/MS of the piperazyl intermediates accumulated in this mutant found molecules having mass formulae corresponding to expected precursors of the left and right sides of petrichorin A (ZR1 and ZR2, Fig. 5B & E) which feature chloro-tryptophan residues in place of chloro-HPIC, in agreement with our predictions.

We found that deleting *ItzS* led to the production of petrichorin C, which was initially discovered in this work after accumulating in our $\triangle ItzD$ NRPS mutant (Fig 4). In contrast with the *ItzD* mutant [unable to synthesize the left cyclopeptide chain of petrichorin A and the entirety of petrichorin B], mutating *ItzS* led to concomitant accumulation of an additional molecule (ZS2) having a mass formula equivalent to the predicted left cyclohexapeptide of the petrichorin A dimer [Fig. 5C & F]. Accordingly, ZS2 was then also posited to be structurally equivalent to the cyclopeptide monomer that is dimerized to create petrichorin B. Finally, deleting *ItzH* led to the production of biosynthetic intermediates with masses that correspond to petrichorin A missing a lone piz- hydroxyl group, or petrichorin B lacking both piz- hydroxyl decorations [Fig. 5D & G; ZH1 and ZH2 respectively, where ZH2 is potentially identical to chloptosin C(53)]. Importantly,

all of these P450 were genetically complemented to restore petrichorin A and B, indicating the accumulated intermediates were not influenced by transcriptional polarity (Fig. S56). Taken together, these data offer strong evidence for *ltz*-locus P450 function that is congruent with our phylogenetic analysis.

345

346

347

348

349

350

351

352

353

354

355

356

357

358

359

360

361

362

363

364

365

366

367

368

369

370

Analysis of petrichorin regulation. Many actinomycete BGCs encode for cluster-situated regulators (CSRs), proteins that function to coordinate transcriptional regulation of the genes in their cluster neighborhood (55). The BGCs encoding for himastatin and the kutznerides both encode CSRs (31, 47), but appear to employ dissimilar regulatory strategies based on a lack of contextually conserved regulatory proteins between them. Xie et al found that himastain biosynthetic regulation is complex, suggesting two canonical transcriptional regulators encoded within the compound's BGC (HmtA and HmtD) are chiefly involved (56). These proteins respectively belong to the MerR and ParB regulatory families, which contrasts with the single SARP-family transcriptional regulator (KtzK) encoded within the core of the kutzeride BGC. Comparing the Itz locus against these clusters revealed a single SARP-encoding gene (ItzP), suggesting closer regulatory parallels with the kutzneride locus. While kutzneride regulation remains experimentally uncharacterized, deleting ItzP led to the complete loss of petrichorin production (JV755, Fig. S57), as well as any LC/MS/MS detectable piperazyl intermediates, supporting the idea that LtzP encodes for an essential petrichorin regulator. The mutant was rescued by ItzP ectopic expression (JV825), but not kutzneride homolog ktzK (JV826), suggesting these regulators have host-specific functions, possibly stemming from different regulator-DNA sequence tropisms.

Himastatin regulatory analyses also suggested that *hmtB*, encoding an acetylglutamate kinase type protein may act as a metabolic regulator (56). While the *ltz* locus lacks a homolog of this protein, we found that deleting *ltzB* (encoding a protein similar to acyl-CoA oxidoreductases) led to the complete abrogation of petrichorin production and any detectable intermediates (Fig. S57). Similar to the *ltzP* regulatory phenotype above, this suggested the *ltz*

locus may also employ metabolic regulatory mechanisms (similar to that inferred for hmtB). Ectopic expression of ItzB weakly rescued the $\Delta ItzB$ phenotype, indicating that polarity isn't likely causal (Fig. S57).

371

372

373

374

375

376

377

378

379

380

381

382

383

384

385

386

387

388

389

390

391

392

393

394

395

396

Interestingly, Ma et al found that deleting the ltzB homolog encoded within the himastatin locus (hmtG) led to complete compound loss, leading those authors to speculate that hmtG may be involved in piz production (31). Because piz biosynthesis is now solved, this explanation seems less likely. However, the strong phenotypes accompanying LtzB/HmtG loss indicates a critical role must exist. Interestingly, both proteins are encoded within syntenic cassettes, characterized an NRPS gene encoding a predicted X-A-T domain arrangement (ItzA/ hmtF), an acyl-CoA oxidoreductase (ItzB/hmtG), then a type II thioesterase (ItzC/hmtH). This conserved arrangement, in combination with our proposed functions for LtzA, led us to infer that LtzB/HmtG proteins may be involved in modulating NRPS protein-protein interactions or a related role. How the oxidoreductase functionality of these proteins might integrate into such a system also needs investigation, but trans-acting proteins are widely known to modulate NRPS assembly lines, including MbtH- type proteins (57) (encoded by ItzG in the petrichorin locus). Petrichorin Cytotoxicity Assays. The dimeric cyclo(depsi)peptides chloptosin, himastatin and enzymatically cross-linked alboflavusins show compelling cytotoxicity profiles (30, 32, 58), and their structural parallels with the petrichorins suggested the latter compounds may have similar properties. Thus, petrichorin A was evaluated for anti-proliferative activity against multiple cancer cell lines. Naturally-heterodimeric petrichorin A was active against A2780 human ovarian cancer, HT1080 fibrosarcoma, the PC3 human prostate cancer, and the Jurkat human T lymphocyte cell lines (a model for acute T cell leukemia) with IC₅₀ values in the range of 20-36 nM. Petrichorins B and C were also active, but to a generally lower extent than petrichorin A. Homodimeric petrichorin B inhibited the four cell lines with IC₅₀ values of 35-73 nM, while monomeric petrichorin C was the least active with IC50 values ranging from 73 to 274 nM (versus paclitaxel control, Table 1 and Fig. S58). Prior alboflavusin monomer vs dimer structure-activity studies (32) led us to predict that monomeric petrichorin C would likely be less active than dimeric petrichorins A and B. However, because homodimers are far more common versus heterodimeric compounds in the context of polyvalent drug development (59), observing that petrichorin A is generally more active than petrichorin B was somewhat surprising. This suggests aryl-crosslinked cyclopeptide heterodimers like petrichorin A, whether encoded by nature or synthesized in a directed way, should be closely considered for future polyvalent molecular diversification and design.

Conclusions:

Actinomycetes are a valued source of biologically active compounds. However, there is a recognized historical bias in how these organisms have been prosecuted for pharmaceutical discovery, with infrequently-encountered "rare actinomycetes" remaining less-explored. The problem of molecule rediscovery is one of several significant reasons quoted to explain why large pharmaceutical companies mostly withdrew from actinomycete -based drug discovery programs (7). However, facing a broadly recognized need for new anti-infectives and other drugs, rare actinomycetes remain relatively fertile for the discovery of novel medicines (24). Despite their perceived value, the biotechnological exploitation of rare-actinomycetes can be challenging. Compared to more-common *Streptomyces*, are fewer strains in cultivation and they often suffer from less-developed genetic toolsets for genome engineering and other important manipulations.

In an effort to discover new bioactive compounds from rare actinomycetes, we designed and tested a bottom-up discovery approach for the targeted metabologenomic identification of yet- undiscovered piperazyl natural products produced by *L. flaviverrucosa*. The recent discovery of the *Streptomyces* incarnatapeptin piperazyl-peptides via a combined *pzbB* mining - ¹⁵N NMR discovery program (60) demonstrates the power of metabologenomics for targeted piperazyl molecule discovery. This work adds to prior efforts by devising a high-throughput

adaptable MS/MS-based approach in place of NMR as a primary screening tool, while also demonstrating that often-used *Streptomyces* genetic toolsets are transferrable to *L. flaviverrucosa*.

Biosynthetic superclusters are chromosomally-adjacent biosynthetic loci that often direct the production of synergistic pairs of molecules. This synergy results in complex pathway inhibition and robust bioactivity profiles for producing organisms [for a recent review, see (61)]. Here, the main product of petrichorin supercluster [petrichorin A] is a pair structurally distinct cyclopeptides that are crosslinked by cytochrome P450 LtzS. LtzS is apparently versatile; being essential for heterodimeric petrichorin A but it also catalyzes minor homodimeric [petrichorin B] chloro-biaryl cyclopeptide crosslinking. While Guo *et al* recently reported the use of related P450s for homodimeric HPIC- piperazyl cyclopeptide crosslinking to bioengineer new cytotoxic homodimers (32), our findings now highlight enzymes within the LtzS/ClpS/HmtS clade for (chloro)biaryl- heterodimer catalysis as well. This suggests additional clade-members could be sought for diversifying HPIC-cyclopeptides via hetero-mulitimerization.

Several mechanisms are suggested to explain why polyvalent molecules, often symmetric homodimers or higher-order mulitimers, have superior biological activities against monomeric analogs (egs. (59, 62-64)). Given this, the substantive bioactivity activity seen for bilaterally-asymmetric petrichorin A [especially in comparison to symmetric petrichorin B] is intriguing and should inspire future heterodimer structure-activity relationship and mechanistic research against additional cell lines and organisms. In sum, this study provides a framework for the exploration and directed biosynthesis of asymmetric cyclopeptide heterodimers, illustrates the utility of a mass-spectrometric-based metabologenomics approach for desirable piperazates, and highlights *L. flaviverrucosa* as a rare actinomycete amenable to manipulation for biotechnological development.

Material and Methods:

Materials. All standard laboratory chemicals were purchased from Sigma-Aldrich, Fisher Scientific, or Santa Cruz Biotechnology. Microbiological media ingredients were purchased from DIFCO. d^7 -L-ornithine was purchased from C/D/N Isotopes and L-piperazic acid dihydrochloride was synthesized and purchased from WuXi AppTec. The publicly available genome sequence of L. flaviverrucosa (GenBank PRJNA463399) was used to guide these studies (ItzA-ItzU; RDI25332.1- RDI25353.1 respectively). See Table S10 for the oligonucleotides used in this study. Growth and Strains. Lentzea flaviverrucosa DSM 44664 was routinely propagated on ISP2 agar (International Streptomyces Project Medium 2, Difco) and TSB (Trypticase Soy Broth, Difco) at 28 °C. Colony PCR templates were prepared by grinding a colony in 100 µL DMSO, essentially as noted elsewhere (65). Escherichia coli was routinely propagated on LB (Lysogeny Broth) Agar and broth at 37 °C according to standard methods. Tables S11 and S12 list plasmids and strains used in this work. For details on intergenic conjugation, and deletion mutant construction, and bioactivity assays (essentially as in (66-71)), see the SI Appendix.

Petrichorin detection. *L flaviverrucosa* colonies were used to inoculate 15 mL of TSB liquid media in a 125-mL Erlenmeyer flask equipped with 6 mm glass beads and vigorous shaking at 28 °C. After 2 d of growth, the culture was plated on ATCC172 (American Type Culture Collection Medium 172) and incubated at 28 °C for 4 d. During initial petrichorin discovery, SMMS agar (72) was also used to afford a less complex LC/MS background signal. After growth, solid agar with adherent cells was chopped into pieces and immersed in ethyl acetate overnight. The resulting extract was evaporated under vacuum and the extract was suspended in 500 μL of HPLC-grade methanol. Methanolic suspensions were syringe filtered (Agilent Captiva Econo Filter, 0.2 μL) before LC/MS analysis. This was performed using a Phenomenex Luna C18 column (75 x 3 mm, 3 μm pore size) installed on an Agilent 1260 Infinity HPLC connected in-line to an Agilent 6420 Triple-Quad mass spectrometer using the following method: T = 0, 10% B; T

= 5, 10% B; T = 25, 100% B; T = 27, 100% B, T = 29, 10% B, T = 30, 10% B; A: water + 0.1% formic acid, B: acetonitrile + 0.1% formic acid; 0.6 mL/min. 10 µL of the methanol-dissolved extract was injected per run, and a total ion count chromatogram was obtained for each sample. Electrospray ionization was used, with MS/MS collision voltage set to 80 V for cyclic petrichorins with product ion scanning as noted in text. Mass filtering between m/z 1300 to 1700 was used to detect intact petrichorin congeners; lower mass bounds were utilized when analyzing biosynthetic intermediates to reduce background signals. For L-piz labeling, a stock solution of 25 mg/mL L-piperazic acid 2HCl was filter sterilized and diluted to the desired concentrations with purified water. 200 µL of the working stock was spread on each ATCC172 plate and allowed to dry before 200 µL of overnight *L. flaviverrucosa* cultures were spread. The calculated concentrations used in agar plates were 10, 50, 100, 500, and 1000 µM. The plates were incubated at 28 °C for 4 d, then the agar with cells was extracted with ethyl acetate overnight. The ethyl acetate was evaporated under vacuum and crude extracts were resuspended in 500 μL methanol and syringe-filtered before analysis. General Chemistry. Optical rotations were measured with a Rudolph Research Analytical Autopal IV Automatic polarimeter. UV and IR spectra were obtained with Shimadzu UV-1800 spectrophotometer and ThermoScientific Nicolet iS50FT-IR spectrometer, respectively. NMR spectra were recorded in Acetone- d_6 with 2 drops of DMSO- d_6 on Varian Unity Inova 500 MHz and Bruker 400 MHz; High resolution mass spectra were obtained an Agilent Q-TOF Ultima ESI-TOF mass spectrometer. Preparative HPLC was carried out on a ThermoScientific U3000 LC system. Extensive multidimensional NMR supporting data are found in the SI Appendix. Isolation of compounds petrichorins A-C. Lentzea flaviverrucosa DSM 44664 was cultured on ATCC172 agar plates at 28 °C for 5 d. The ethyl acetate (EtOAc) crude extract (1.41 g) was subjected to preparative HPLC (phenyl-hexyl column, 5 µm; 100.0 × 21.2 mm; 10 mL/min; with 0.1% formic acid in mobile phases) eluted with 20%-100% acetonitrile/H₂O in 40 min to obtain 40 fractions (SF.1-40). F17 (57.2 mg) and F18 (32.8 mg) were further separated by semi-

475

476

477

478

479

480

481

482

483

484

485

486

487

488

489

490

491

492

493

494

495

496

497

498

499

500

preparative HPLC (C18 column, 5 μ m; 250.0 mm × 10.0 mm; 4 mL/min; with 0.1% formic acid in 78% CH₃OH/H₂O) to yield petrichorin A (35.7 mg, t_R 11.4 min) and petrichorin B (3.61 mg, t_R 14.7 min), respectively. Mutant strain JV757 (Δ ItzD) was also cultured on 5 L equivalent of ATCC172 media agar plates at 28 °C for 6 d. The EtOAc crude extract (471.28 mg) was subjected to preparative HPLC (phenyl-hexyl column, 5 μ m; 100.0 × 21.2 mm; 10 mL/min; with 0.1% formic acid in mobile phases) eluted with 20%-100% methanol/H₂O in 35 min to get 35 fractions (F1-35). All the fractions were analyzed by LC-MS and the target compound with the molecule weight of 717 Da was detected in F28. Further separation of F28 (9.68 mg) with semi-preparative HPLC (C18 column, 5 μ m; 250.0 mm × 10.0 mm; 4 mL/min; 20-40% CH₃CN/H₂O in 60 min) led to the isolation of petrichorin C (3.25 mg, t_R 28.5 min). Details on the hydrolysis and analysis of the petrichorins via Marfey (Table S13) and Mosher derivatization (essentially as previously described (73, 74)) are in the SI Appendix. Also see SI appendix for details of DP4 NMR calculations (75).

- Acknowledgments. This work was supported by the Hawaii Community Foundation (15ADVC-
- 516 74420, 17CON-86295, and 20CON-102163), and the Hawaii IDeA Network for Biomedical
- 517 Research Excellence III and IV (INBRE-III and INBRE-IV) project (NIGMS Grant
- 518 5P20GM103466) to SC. It was also supported by NSF-CAREER 1846005 to JAVB. The authors
- thank Lee Douangkeomany for assistance with *Lentzea* mutagenesis.
- **Contributions**:
- 521 J. A. V. B. and S. C. conceived the project. C. L., Y. H., X. U., S. D. S., Y. Q., J. M. D., K. K. N.,
- and A. M. S. performed experiments. All authors analyzed data. C. L, Y. H., A. M. S., S. C.,
- and J. A. V. B. wrote the manuscript.

524 Competing Interest Statement:

No competing interests.

References:

526

- 527 1. A. T. Bull, A. C. Ward, M. Goodfellow, Search and discovery strategies for biotechnology: the paradigm shift. *Microbiology and Molecular Biology Reviews* **64**, 573-606 (2000).
- 529 2. M. I. Hutchings, A. W. Truman, B. Wilkinson, Antibiotics: past, present and future. *Current Opinion in Microbiology* **51**, 72-80 (2019).
- 3. R. H. Baltz, Renaissance in antibacterial discovery from actinomycetes. *Current opinion in Pharmacology* **8**, 557-563 (2008).
- 4. A. G. Atanasov, S. B. Zotchev, V. M. Dirsch, C. T. Supuran, Natural products in drug discovery: Advances and opportunities. *Nature Reviews Drug Discovery* **20**, 200-216 (2021).
- 535 5. M. L. Cohen, Changing patterns of infectious disease. *Nature* **406**, 762-767 (2000).
- 536 6. L. Katz, R. H. Baltz, Natural product discovery: past, present, and future. *Journal of Industrial Microbiology and Biotechnology* **43**, 155-176 (2016).
- 7. R. H. Baltz, Genome mining for drug discovery: progress at the front end. *Journal of Industrial Microbiology and Biotechnology* kuab044, https://doi.org/10.1093/jimb/kuab044 (2021).
- 8. B. O. Bachmann, S. G. Van Lanen, R. H. Baltz, Microbial genome mining for accelerated natural products discovery: is a renaissance in the making *Journal of Industrial Microbiology and Biotechnology* **41**, 175-184 (2014).
- 543 9. D. W. Udwary, H. Otani, N. J. Mouncey, New keys to unlock the treasure trove of microbial natural products. *Nature Reviews Microbiology*, 1-1 doi: 10.1038/s41579-021-00631-7. (2021).
- 545 10. P. A. Hoskisson, R. F. Seipke, Cryptic or silent? The known unknowns, unknown knowns, and unknown unknowns of secondary metabolism. *MBio* **11**, e02642-02620 (2020).
- J.-L. Wolfender, M. Litaudon, D. Touboul, E. F. Queiroz, Innovative omics-based approaches for prioritisation and targeted isolation of natural products—new strategies for drug discovery.
 Natural Product Reports 36, 855-868 (2019).
- 550 12. O. N. Sekurova, O. Schneider, S. B. Zotchev, Novel bioactive natural products from bacteria via 551 bioprospecting, genome mining and metabolic engineering. *Microbial Biotechnology* **12**, 828-552 844 (2019).
- 553 13. M. A Ciufolini, N. Xi, Synthesis, chemistry and conformational properties of piperazic acids. 554 *Chemical Society Reviews* **27**, 437-439 (1998).
- 555 14. M. E. Welsch, S. A. Snyder, B. R. Stockwell, Privileged scaffolds for library design and drug discovery. *Current Opinion In Chemical Biology* **14**, 347-361 (2010).
- 15. E. L. Handy, J. K. Sello, "Structure and Synthesis of Conformationally Constrained Molecules
 Containing Piperazic Acid". (Springer Berlin Heidelberg, Berlin, Heidelberg, 2015),
 10.1007/7081 2015 185, pp. 1-29.
- 560 16. W. Jiang *et al.*, Biosynthetic chlorination of the piperazate residue in kutzneride biosynthesis by KthP. *Biochemistry* **50**, 6063-6072 (2011).
- 562 17. Y.-L. Du, H.-Y. He, M. A. Higgins, K. S. Ryan, A heme-dependent enzyme forms the nitrogen— 563 nitrogen bond in piperazate. *Nature Chemical Biology* **13**, 836 (2017).
- 564 18. Y. Hu, Y. Qi, S. D. Stumpf, J. M. D'Alessandro, J. A. V. Blodgett, Bioinformatic and functional evaluation of actinobacterial piperazate metabolism. *ACS Chemical Biology* **14**, 696-703 (2019).
- 566 19. C. S. Sit *et al.* Variable genetic architectures produce virtually identical molecules in bacterial symbionts of fungus-growing ants. *Proceedings of the National Academy of Sciences of the United States of America*, **112**, 13150-13154 (2015).
- 569 20. D.-C. Oh, M. Poulsen, C. R. Currie, J. Clardy, Dentigerumycin: a bacterial mediator of an antfungus symbiosis. *Nature Chemical Biology* **5**, 391-393 (2009).
- 571 21. D. Shin *et al.*, Coculture of marine *Streptomyces* sp. with *Bacillus* sp. produces a new piperazic acid-bearing cyclic peptide. *Frontiers in Chemistry* **6**, 498 (2018).

- 573 22. K. D. Morgan, R. J. Andersen, K. S. Ryan, Piperazic acid-containing natural products: structures and biosynthesis. *Natural Product Reports* **36**, 1628-1653 (2019).
- 575 23. M. Goodfellow, I. Nouioui, R. Sanderson, F. Xie, A. T. Bull, Rare taxa and dark microbial matter: 576 novel bioactive actinobacteria abound in Atacama Desert soils. *Antonie van Leeuwenhoek* **111**, 577 1315-1332 (2018).
- 578 24. K. Tiwari, R. K. Gupta, Rare actinomycetes: a potential storehouse for novel antibiotics. *Critical Reviews in Biotechnology* **32**, 108-132 (2012).
- 580 25. K. Pommerehne, J. Walisko, A. Ebersbach, R. Krull, The antitumor antibiotic rebeccamycin—
 581 challenges and advanced approaches in production processes. *Applied Microbiology and Biotechnology* 103, 3627-3636 (2019).
- 583 26. H. Lee, J.-W. Suh, Anti-tuberculosis lead molecules from natural products targeting
 584 *Mycobacterium tuberculosis* ClpC1. *Journal of Industrial Microbiology and Biotechnology* 43,
 585 205-212 (2016).
- 586 27. D. Wichner *et al.*, Isolation and anti-HIV-1 integrase activity of lentzeosides A–F from 587 extremotolerant *Lentzea* sp. H45, a strain isolated from a high-altitude Atacama Desert soil. *The* 588 *Journal of Antibiotics* **70**, 448-453 (2017).
- 589 28. S. Sasamura *et al.*, Bioconversion of FR901459, a novel derivative of cyclosporin A, by *Lentzea* sp. 7887. *The Journal of Antibiotics* **68**, 511-520 (2015).
- 591 29. W. Tao *et al.*, A genomics-led approach to deciphering the mechanism of thiotetronate antibiotic biosynthesis. *Chemical Science* **7**, 376-385 (2016).
- 593 30. K. Umezawa, Y. Ikeda, Y. Uchihata, a. Hiroshi Naganawa, S. Kondo, Chloptosin, an Apoptosis-594 Inducing Dimeric Cyclohexapeptide Produced by Streptomyces. *The Journal of Organic* 595 *Chemistry* **65**, 459–463 (1999).
- J. Ma *et al.*, Biosynthesis of Himastatin: Assembly Line and Characterization of Three
 Cytochrome P450 Enzymes Involved in the Post-tailoring Oxidative Steps. *Angewandte Chemie International Edition* 50, 7797-7802 (2011).
- Z. Guo *et al.*, Design and biosynthesis of dimeric alboflavusins with biaryl linkages via
 regiospecific C–C bond coupling. *Journal of the American Chemical Society* **140**, 18009-18015
 (2018).
- 33. Z. Guo *et al.*, NW-G01, a novel cyclic hexapeptide antibiotic, produced by *Streptomyces* alboflavus 313: II. Structural elucidation. *Journal of Antibiotics (Tokyo)* 63, 231-235 (2010).
- A. Broberg, A. Menkis, R. Vasiliauskas, Kutznerides 1-4, depsipeptides from the actinomycete Kutzneria sp. 744 inhabiting mycorrhizal roots of *Picea abies* seedlings. *Journal Of Natural* Products **69**, 97-102 (2006).
- T. Ogita *et al.*, Matlystatins, new inhibitors of typeIV collagenases from *Actinomadura* atramentaria. I. Taxonomy, fermentation, isolation, and physico-chemical properties of matlystatin-group compounds. *Journal of Antibiotics (Tokyo)* **45**, 1723-1732 (1992).
- F. Leipoldt *et al.*, Warhead biosynthesis and the origin of structural diversity in hydroxamate metalloproteinase inhibitors. *Nature Communications* **8**, 1-12 (2017).
- 612 37. K. C.-C. Cheng *et al.*, Actinoramide A identified as a potent antimalarial from titration-based screening of marine natural product extracts. *Journal of Natural Products* **78**, 2411-2422 (2015).
- S. Cao *et al.*, Ipomoeassins A– E, Cytotoxic Macrocyclic Glycoresins from the Leaves of *Ipomoea* squamosa from the Suriname Rainforest. *Journal of Natural Products* **68**, 487-492 (2005).
- N. Grimblat, A. M. Sarotti, Computational chemistry to the rescue: Modern toolboxes for the
 assignment of complex molecules by GIAO NMR calculations. *Chemistry—A European Journal* 22,
 12246-12261 (2016).

- N. s. Grimblat, J. A. Gavín, A. Hernández Daranas, A. M. Sarotti, Combining the power of J coupling and DP4 analysis on stereochemical assignments: the J-DP4 methods. *Organic Letters* 21, 4003-4007 (2019).
- N. s. Grimblat, M. M. Zanardi, A. M. Sarotti, Beyond DP4: an improved probability for the
 stereochemical assignment of isomeric compounds using quantum chemical calculations of
 NMR shifts. The Journal of Organic Chemistry 80, 12526-12534 (2015).
- 42. T. A. Lundy, S. Mori, S. Garneau-Tsodikova, A thorough analysis and categorization of bacterial
 interrupted adenylation domains, including previously unidentified families. *RSC Chemical Biology* 1, 233-250 (2020).
- 43. L. M. Alkhalaf, K. S. Ryan, Biosynthetic manipulation of tryptophan in bacteria: pathways and mechanisms. *Chemistry & Biology* **22**, 317-328 (2015).
- 630 44. H. Luhavaya, R. Sigrist, J. R. Chekan, S. M. McKinnie, B. S. Moore, Biosynthesis of I-4-
- chlorokynurenine, an antidepressant prodrug and a non-proteinogenic amino acid found in lipopeptide antibiotics. *Angewandte Chemie International Edition* **131**, 8482-8487 (2019).
- 633 45. C. Dong *et al.*, Tryptophan 7-halogenase (PrnA) structure suggests a mechanism for regioselective chlorination. *Science* **309**, 2216-2219 (2005).
- M. Bernhardt, S. Berman, D. Zechel, A. Bechthold, Role of Two Exceptional trans Adenylation
 Domains and MbtH-like Proteins in the Biosynthesis of the Nonribosomal Peptide WS9324A
- from Streptomyces calvus ATCC 13382. ChemBioChem **21**, 2659 (2020).
- D. G. Fujimori *et al.*, Cloning and characterization of the biosynthetic gene cluster for kutznerides. *Proceedings of the National Academy of Sciences of the United States of America* 104, 16498-16503 (2007).
- 48. Q. Li *et al.*, Deciphering the biosynthetic origin of L-*allo*-isoleucine. *Journal of the American Chemical Society* **138**, 408-415 (2016).
- 49. J. Liu *et al.*, Biosynthesis of the Anti-infective Marformycins Featuring Pre-NRPS Assembly Line
 644 N-Formylation and O-Methylation and Post-Assembly Line C-Hydroxylation Chemistries. Organic
 645 Letters 17, 1509-1512 (2015).
- P. Ruiz Sanchis, S. A. Savina, F. Albericio Palomera, M. Álvarez Domingo, Structure, bioactivity
 and synthesis of natural products with hexahydropyrrolo [2, 3-b] indole. *Chemistry-A European Journal* 17, 1388-1408 (2011).
- 51. J. D. Rudolf, C.-Y. Chang, M. Ma, B. Shen, Cytochromes P450 for natural product biosynthesis in 550 Streptomyces: sequence, structure, and function. *Natural Product Reports* **34**, 1141-1172 (2017).
- 52. D. Sirim, F. Wagner, A. Lisitsa, J. Pleiss, The cytochrome P450 engineering database: Integration of biochemical properties. *BMC Biochemistry* **10**, 1-4 (2009).
- H. Hashizume *et al.*, New chloptosins B and C from an *Embleya* strain exhibit synergistic activity
 against methicillin-resistant *Staphylococcus aureus* when combined with co-producing
 compound L-156,602. *The Journal of Antibiotics* 74, 80-85 (2021).
- 54. J. G. Owen *et al.*, Mapping gene clusters within arrayed metagenomic libraries to expand the
 structural diversity of biomedically relevant natural products. *Proceedings of the National Academy of Sciences* 110, 11797-11802 (2013).
- 659 55. G. Liu, K. F. Chater, G. Chandra, G. Niu, H. Tan, Molecular regulation of antibiotic biosynthesis in 660 Streptomyces. Microbiology and Molecular Biology Reviews **77**, 112-143 (2013).
- 56. Y. Xie, Q. Li, X. Qin, J. Ju, J. Ma, Enhancement of himastatin bioproduction via inactivation of
 atypical repressors in *Streptomyces hygroscopicus*. *Metabolic Engineering Communications* 8,
 e00084 (2019).

- 57. E. A. Felnagle *et al.*, MbtH-like proteins as integral components of bacterial nonribosomal peptide synthetases. *Biochemistry* **49**, 8815-8817 (2010).
- 58. K. S. LAM *et al.*, Himastatin, a new antitumor antibiotic from *Streptomyces hygroscopicus* I.
 Taxonomy of producing organism, fermentation and biological activity. *The Journal of Antibiotics* 43, 956-960 (1990).
- A. Greer, O. R. Wauchope, N. S. Farina, P. Haberfield, J. F. Liebman, Paradigms and paradoxes:
 Mechanisms for possible enhanced biological activity of bilaterally symmetrical chemicals.
 Structural Chemistry 17, 347-350 (2006).
- 672 60. K. D. Morgan *et al.*, Incarnatapeptins A and B, Nonribosomal Peptides Discovered Using Genome 673 Mining and 1H/15N HSQC-TOCSY. *Organic Letters* **22**, 4053-4057 (2020).
- 674 61. K. J. Meyer, J. R. Nodwell, Biology and applications of co-produced, synergistic antimicrobials from environmental bacteria. *Nature Microbiology* **6**, 1118-1128 (2021).
- 676 62. H. Aldemir, R. Richarz, T. A. Gulder, The biocatalytic repertoire of natural biaryl formation.

 677 *Angewandte Chemie International Edition* **53**, 8286-8293 (2014).
- 678 63. C. Chittasupho, Multivalent ligand: design principle for targeted therapeutic delivery approach.

 77 Therapeutic Delivery 3, 1171-1187 (2012).
- 680 64. J. H. Griffin *et al.*, Multivalent drug design. Synthesis and in vitro analysis of an array of vancomycin dimers. *Journal of the American Chemical Society* **125**, 6517-6531 (2003).
- 682 65. W. Van Dessel, L. Van Mellaert, N. Geukens, J. Anné, Improved PCR-based method for the direct screening of *Streptomyces* transformants. *Journal of Microbiological Methods* **53**, 401-403 (2003).
- 685 66. J. A. V. Blodgett *et al.*, Unusual transformations in the biosynthesis of the antibiotic phosphinothricin tripeptide. *Nature Chemical Biology* **3**, 480-485 (2007).
- 687 67. Y. Qi, E. Ding, J. A. Blodgett, Native and engineered clifednamide biosynthesis in multiple 688 Streptomyces spp. ACS Synthetic Biology **7**, 357-362 (2017).
- 689 68. B. Ko *et al.*, Construction of a new integrating vector from actinophage φOZJ and its use in
 690 multiplex *Streptomyces* transformation. *Journal of Industrial Microbiology and Biotechnology* **47**,
 691 73-81 (2020).
- 69. J. A. V. Blodgett *et al.*, Common biosynthetic origins for polycyclic tetramate macrolactams from
 693 phylogenetically diverse bacteria. *Proceedings of the National Academy of Sciences of the United* 694 *States of America* 107, 11692-11697 (2010).
- 695 70. A. Delazar *et al.*, Iridoid glycosides from *Eremostachys glabra*. *Journal of Natural Products*. **67**, 696 1584-1587 (2004).
- 5. Cao *et al.*, Cytotoxic and other compounds from *Didymochlaena truncatula* from the Madagascar rain forest. *Journal of Natural Products* **69**, 284-286 (2006).
- 72. T. Keiser, M. Bibb, M. Buttner, K. Chater, D. Hopwood, *Practical Streptomyces Genetics* (The John Innes Foundation, Norwich, 2000).
- 73. K. C. Cheng *et al.*, Actinoramide A Identified as a Potent Antimalarial from Titration-Based
 Screening of Marine Natural Product Extracts. *Journal of Natural Products* 78, 2411-2422 (2015).
- 703 74. S. Cao *et al.*, Ipomoeassins A-E, cytotoxic macrocyclic glycoresins from the leaves of *Ipomoea* squamosa from the Suriname rainforest. *Journal of Natural Products* **68**, 487-492 (2005).
- 75. C. S. Li *et al.*, NF-kappaB inhibitors, unique gamma-pyranol-gamma-lactams with sulfide and sulfoxide moieties from Hawaiian plant *Lycopodiella cernua* derived fungus *Paraphaeosphaeria neglecta* FT462. *Scientific Reports* **7**, 10424 (2017).

Figure Legends:

708

Figure 1. Actinobacterial piperazyl cyclic(depsi)peptides. *Top*, several naturally-occurring cyclic peptides having HPIC (blue) and piz (red) substituents are known from the literature. Many examples are monomeric, including kutzneride 1 and the alboflavusin congener NW-GO1. Natural homodimers in the class are also known (egs. himastatin and chloptosin). The homodimers are comprised of identical monomers symmetrically coupled via (chloro)biaryl linkages (green darts). *Bottom*, Structures of petrichorins A and B discovered herein. Petrichorin A is heterodimeric; each cyclopeptide half of the chlorobiaryl is structurally-distinct. The left cyclopeptide of petrichorin A is identical to that making up the homodimer petrichorin B. The right cyclopeptide constituent of petrichorin A (grey background) was later identified as a monomer, petrichorin C, that accumulates in certain deletion mutants; see text.

Figure 2. Petrichorin discovery via targeted metabologenomics. (A) Open reading frame map of the *L. flaviverrucosa Itz* locus, a biosynthetic supercluster that encodes for the petrichorins. Piperazate biosynthetic genes *ItzF* and *ItzT* are centrally positioned within the cluster (purple), which is predominantly made up of genes encoding for NRPS enzymology, tailoring and regulatory functions indicated in the color key. (B) UV-HPLC analysis of *L. flaviverrucosa* organic extracts revealed a Piz-responsive peak (#), which (C) also showed evidence of d^7 -*L*-orn incorporation by mass-envelope broadening following MS analysis. Consistent with piperazyl compound biosynthesis (see (C) inset labeling scheme), (D) piperazyl-targeted HPLC-MS/MS revealed same major peak found in panels B & C [#, petrichorin A] plus a minor, later eluting peak [^, petrichorin B]. Both molecules are lost by deleting *ItzT*, and both were rescued by ectopic expression of *ItzT* or its orthologs *ktzT* and *hmtC*. Error bars in (B) indicate Standard Deviation.

Figure 3. Dual NRPS and flavin-dependent chlorinase assembly lines for the cyclopeptide precursors of petrichorin A and B. Note that cytochrome P450-dependent Piz-hydroxylation,

HPIC-maturation and aryl-crosslinking activities needed for precursor maturation and complete petrichorin assembly are excluded; see Figures 4 and 5. The predicted tryptophan chlorinase regiospecificites [LtzN, C6 and LtzM, C7; carbon assignment from (43)] were inferred by protein identity against functionally characterized homologs (44, 45) [LtzN:Tar14, 66%; LtzM:PrnA, 59% identical]. Flavin:nicotinamide cofactor oxidoreductases similar to LtzO often functionally pair with such enzymes. In both NRPS-assembly lines, LtzA is proposed to act *in trans* to compensate for absent adenylation domains in LtzV and LtzE. Standard NRPS domain abbreviations are used (A- adenylation, T- thiolation, E- epimerization, X- unknown function, O-Mt- O-methyltransferase, N-Mt- N-methyltransferase, TE- thioesterase)

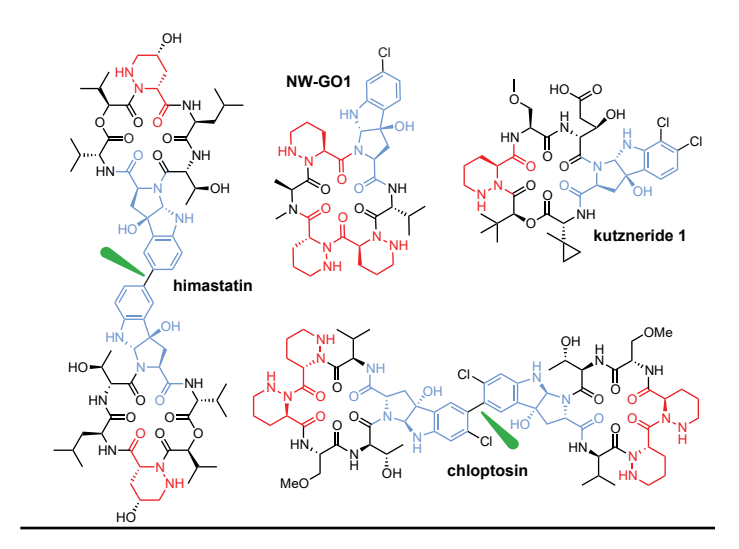
Figure 4. Biosynthetic analysis of petrichorin NRPS gene mutants *ItzD* and *ItzU* via LC/MS/MS.

(A) Deleting *ItzD* caused the loss of petrichorin A and B, with the concomitant accumulation of the monomer petrichorin C. In contrast, deleting (B) *ItzU* abrogated only petrichorin A, while the homodimer petrichorin B continued production. Thus, *ItzU* is essential for petrichorin A production via the petrichorin C intermediate, while *ItzD* is responsible for the cyclopeptide intermediate that is matured into petrichorin B, plus one- half of the petrichorin A heterodimer.

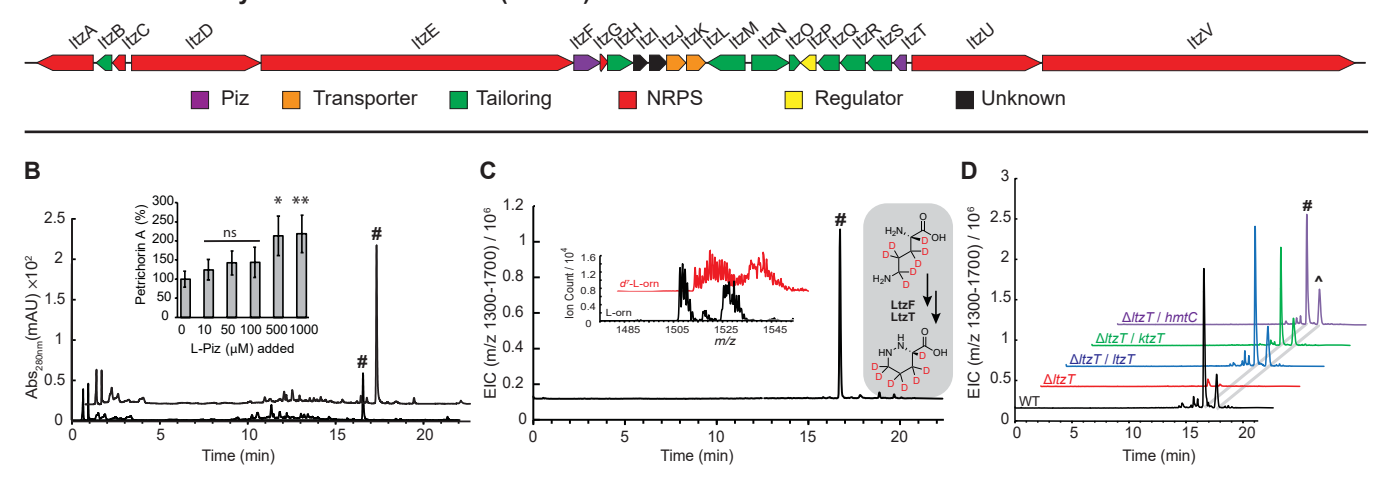
(C) *rpsL* parental control showing the relative retention times of petrichorin A and B.

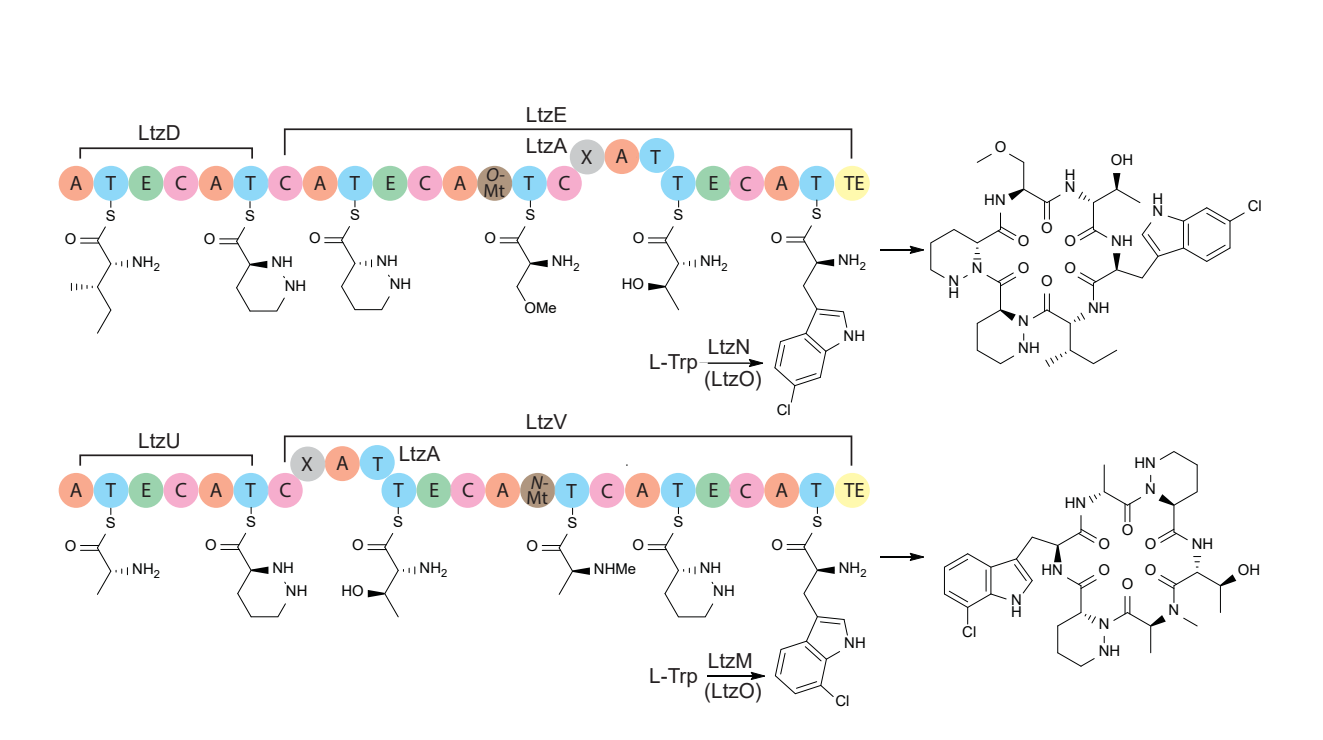
Figure 5. Phylogenetic and metabolic analyses to assign *Itz*-locus cytochrome P450 gene functions. The cytochrome P450s associated with BGCs encoding molecules like those found in Fig. 1 share significant homology and are thus challenging to functionally assign via sequence identity alone (32). However, (A) a maximum-likelihood phylogeny bins P450s involved in HPIC maturation (blue branches) and biaryl-crosslinking (red branches) into monophyletic groups, indicating potential orthology. In contrast, putative piperazyl-hydroxylating P450s (HmtN, LtzH and AfnA) failed to show similar monophyly. CypX [AGS49593.1 (54)], an exemplar CYP113C-family P450, was used as an outgroup; the tree was constructed with 500

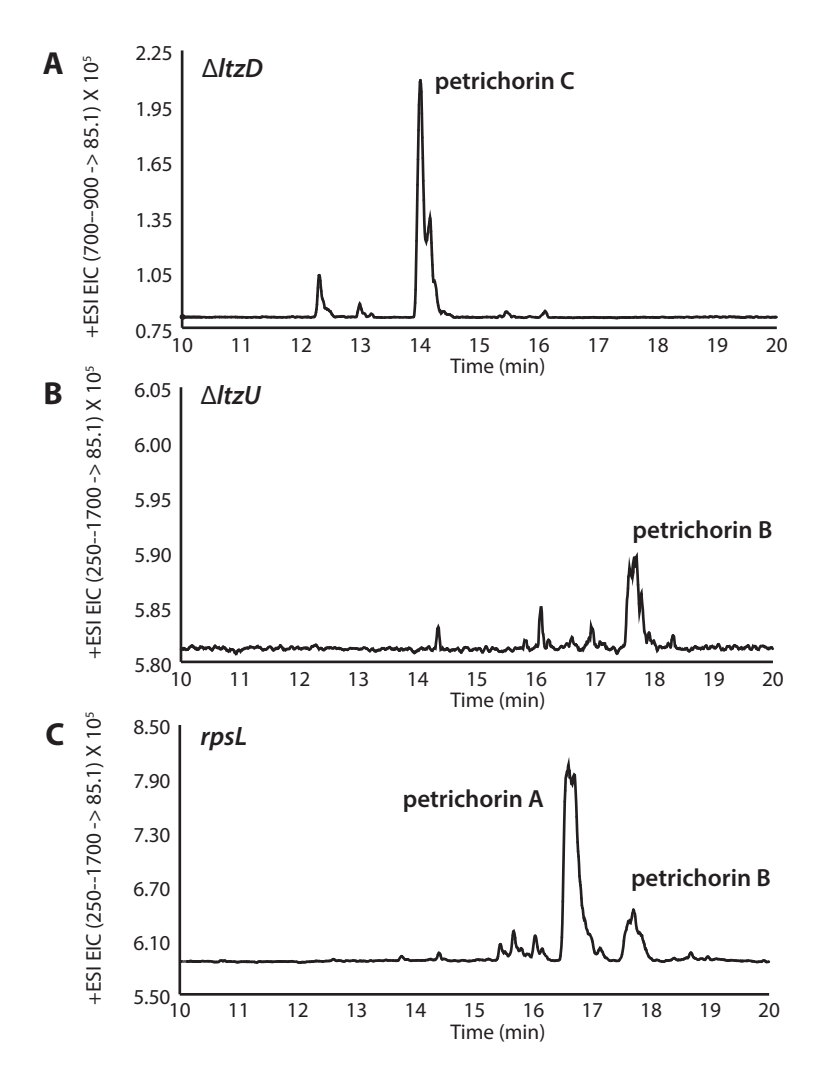
bootstraps and branches <90% confidence were collapsed with actual values noted at nodes. (B-D), LC/MS/MS analysis of biosynthetic intermediates accumulated in *ItzR*, *ItzS* and *ItzH* mutants, respectively, plus (E-G) homology-inferred and HRMS-supported structures of key molecules arising in each mutant. For each proposed intermediate, the shaded circles indicate the target of each P450, with colors matching those used to highlight the tree in (A). Hydroxylation targets are indicated in dark charcoal (G). Several mutants accumulated intermediates having masses commensurate with hydride [2H] or hydroxyl [OH] additions or losses [±] to the illustrated structures; these are denoted within chromatogram peak callouts for clarity. Peak in (C) indicated with * has a mass equivalent with ZS2; indicating a likely geometric isomer thereof.



A Petrichorin Biosynthetic Gene Cluster (~67 kb)







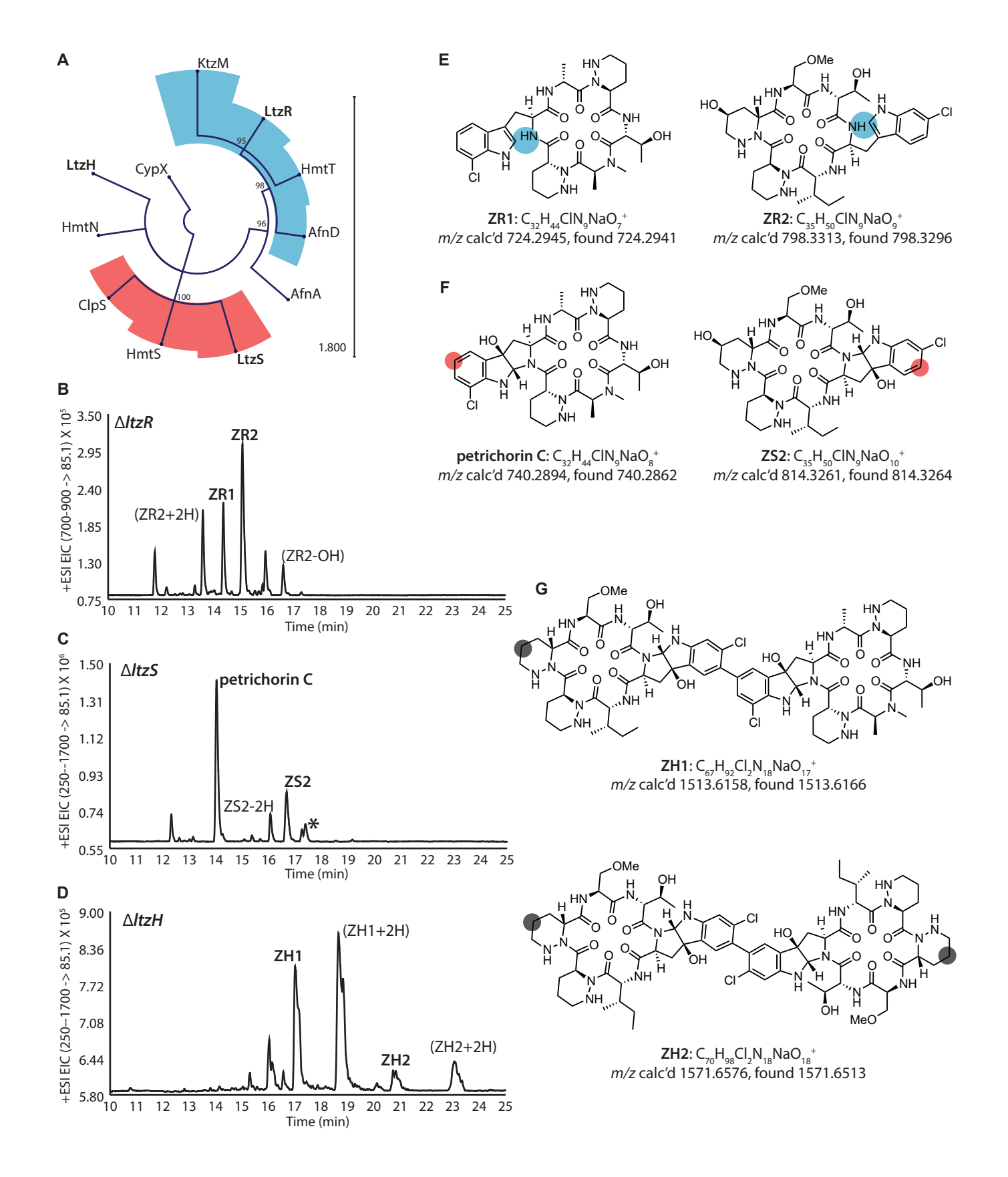


Table 1. Petrichorin IC₅₀ values (nM) against select human cancer cell lines with paclitaxel control

Cell lines	petrichorin A	petrichorin B	petrichorin C	paclitaxel
A2780S	28.12 +/- 2.329	35.32 +/- 4.289	169.14 +/- 2.860	8.127 +/- 2.156
HT1080	35.51 +/- 4.194	36.36 +/- 3.423	72.41 +/- 3.021	75.0 +/- 2.511
PC3	34.49 +/- 2.262	68.43 +/- 3.296	273.46 +/- 3.385	136.0 +/- 1.494
Jurkat	20.25 +/- 2.624	72.47 +/- 1.551	101.9 +/- 3.014	8.694 +/- 2.699